

Nanocrystal-based hybrid white light generation with tunable colour parameters

S Nizamoglu^{1,3} and H V Demir^{1,2,3}

¹ Department of Physics, Bilkent University, Ankara, TR-06800, Turkey

² Department of Electrical and Electronics Engineering, Bilkent University, Ankara, TR-06800, Turkey

³ Nanotechnology Research Center, Bilkent University, Ankara, TR-06800, Turkey

E-mail: volkan@bilkent.edu.tr (H V Demir)

Received 31 January 2007, accepted for publication 28 March 2007

Published 24 August 2007

Online at stacks.iop.org/JOptA/9/S419

Abstract

We present the hybridization of CdSe/ZnS core–shell nanocrystals (NCs) on InGaN/GaN based blue/near-UV LEDs to generate light widely tunable across the visible spectral range and especially within the white region of the CIE (1931) chromaticity diagram. We report on the design, growth, fabrication and characterization of these hybrid NC-LEDs. In 26 NC-LED samples, we experimentally show the effect of the NC concentration and NC film thickness on tuning the colour properties of the generated light (tristimulus coordinates, colour rendering index and correlated temperature) and further compare layer by layer assembly and blending of NCs for integration in LEDs. With greatly tunable colour properties, these hybrid white light sources hold promise for future lighting and display applications.

Keywords: nanocrystals, white light generation, LEDs

(Some figures in this article are in colour only in the electronic version)

Within the next five years, it is likely that white light emitting diodes (WLEDs) will be used for all external lighting functions on vehicles [1]. Because of such wide-scale potential use, WLEDs have attracted both scientific attention and commercial interest [2]. Different approaches for white light generation such as multi-chip WLEDs, monolithic WLEDs and colour-conversion WLEDs have been extensively investigated [3–5]. Among these, multi-chip white LEDs (and monolithic WLEDs, in principle, for the same matter) tend to exhibit higher electrical-to-light conversion efficiencies when compared with colour-conversion WLEDs, for the multi-chip WLEDs do not have additional energy losses caused by the Stokes shift and nonradiative recombination, unlike in the phosphor coating of colour-conversion WLEDs. Additionally, multi-chip WLEDs do not suffer ageing problems related to the phosphor, which affects the lifetime of colour-conversion WLEDs [6]. However, for multi-chip WLEDs, the driving electric circuit is typically comparatively complex for general illumination purposes, leading to increased costs [5]. As a result, the colour-conversion approach provides an advantage specifically in having simple circuits (and thus reduced

cost) when compared to the multi-chip WLED approach. Today, using the colour-conversion technique, phosphor-based WLEDs have been widely commercialized and are currently in use. In phosphor-based colour conversion, however, difficulties in controlling granule size systematically, and mixing and depositing films uniformly pose the most fundamental disadvantages, which result in undesired visible colour variations [7].

As an alternative approach, nanocrystals (NCs) have recently been used for colour conversion in white light generation. To date we have introduced white light generation using CdSe/ZnS core–shell nanocrystals of single, dual, trio and quadruple combinations hybridized with blue InGaN/GaN LEDs [8, 9]. Also, a blue/green two-wavelength InGaN/GaN LED coated with a single type of red NC and a blue InGaN/GaN LED with a single type of yellow NC and a dual type of red and green NCs have been reported [10–12]. In this paper, we present the hybridization of CdSe/ZnS core–shell nanocrystals (NCs) on InGaN/GaN-based blue/near-UV LEDs to generate light widely tunable across the visible spectral range and especially within the white region of the

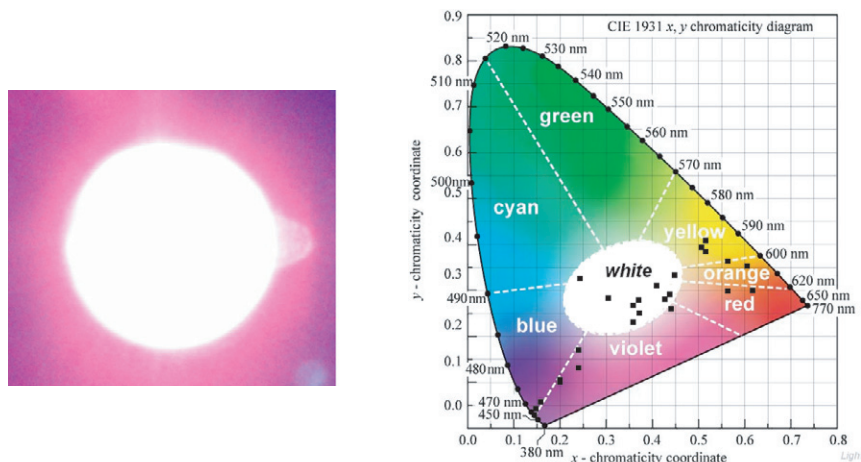


Figure 1. A photograph of white light generation from one of our hybrid white NC-WLEDs (left) and tristimulus coordinates of our hybrid NC-WLEDs on the CIE (1931) chromaticity diagram.

CIE (1931) chromaticity diagram, as shown as an exemplary implementation in figure 1 (left). Here we report on the design, growth, fabrication and characterization of these hybrid NC-LEDs. In 26 of our NC-LED samples, we experimentally show the effect of the NC concentration and NC film thickness on tuning the colour properties of the generated light (tristimulus coordinates, colour rendering index and correlated temperature), as shown on the CIE chromaticity diagram in figure 1 (right). We further compare layer by layer assembly and blending of NCs for integration on LEDs. Using combinations of nanocrystals and organizing them mixed and/or unmixed in layers, we tune the colour parameters of the generated light.

We adjust the colour properties (tristimulus coordinates, correlated colour temperature and colour rendering index) of the generated white light by setting the device parameters including the thickness and order of the NC films and the type and concentration of NCs. The order of NC films, with a different NC type in each film, determines the level of reabsorption of the photons emitted by the preceding NC layers. The film thickness and NC density affect the level of conversion from incident photons to emitted/transmitted photons for each NC layer. The type of NCs determines the intervals of the visible spectrum designed to contribute to white light. Therefore, the ability to control such hybrid device parameters makes it possible to generate the intended white light spectrum in the visible.

We use four types of CdSe/ZnS core-shell NCs from Evident Technologies. Their photoluminescence in the visible spectral range corresponds to cyan, green, yellow and red. The NC diameters range from 1.9 to 5.2 nm. We use these NCs blended in host resin with a size distribution of $\pm 5\%$. We use both PMMA and UV-curable resin to make NC films that enable us to adjust the concentration. When we hybridize the NCs in toluene and host polymer on LEDs, since the toluene solvent evaporates, given the total number of NCs in the solution, the amount of polymer controllably determines the NC concentration. Usually the NC concentration we use for hybridization ranges from 3.04 to 140 nmol/1 ml of resin. We can use NC film thickness ranging from a few micrometre

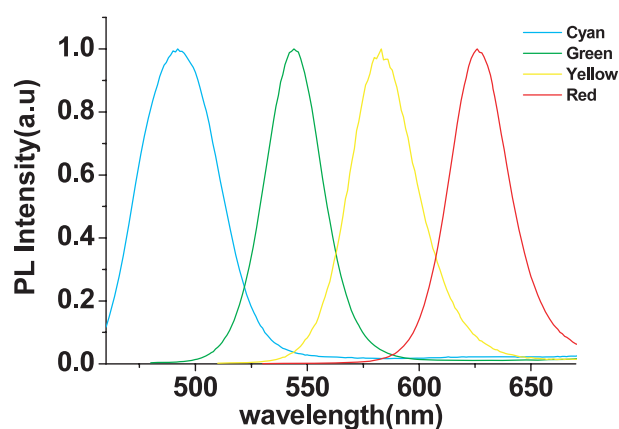


Figure 2. Photoluminescence spectra of our CdSe-ZnS core-shell nanocrystals in host polymer.

to 1700 μm , depending on the concentration of NC film. Our cyan, green, yellow and red NCs exhibit photoluminescence (PL) peaks at 500, 540, 580 and 620 nm, respectively, as characterized at our labs [8] and shown here in figure 2.

We use an n-UV LED and two types of blue InGaN/GaN LEDs for integration. The n-UV LED has a peak electroluminescence at 383 nm, one of the blue LEDs at 440 nm and the other at 452 nm. We use an epitaxial layer design similar for the n-UV LED and the two blue LEDs. The difference between the n-UV and blue LEDs is the epitaxial growth temperatures and the thickness of the active layers (2–3 nm for the n-UV LED and 4–5 nm for the blue LEDs). The difference between the two blue LEDs is only the change of the epitaxial growth temperatures of their respective active layers. The design of these InGaN/GaN LEDs is presented along with the thickness of each epitaxial layer in figure 3.

We use a GaN dedicated metal-organic chemical vapour deposition (MOCVD) system (Aixtron RF200/4 RF-S) for the growth of our epitaxial layers at Bilkent University Nanotechnology Research Center. We start with a 14 nm thick GaN nucleation layer and a 200 nm thick GaN buffer layer to increase the crystal quality of the device epitaxial layers.

120 nm	p+ - GaN
50 nm	p - AlGaIn
4 nm	p - GaN
5 InGaIn/GaN well / barrier	
690 nm	n - GaN
200 nm	GaN
14 nm	GaN
sapphire	

Figure 3. Epitaxial structure of our blue LEDs (not drawn to scale) [8].

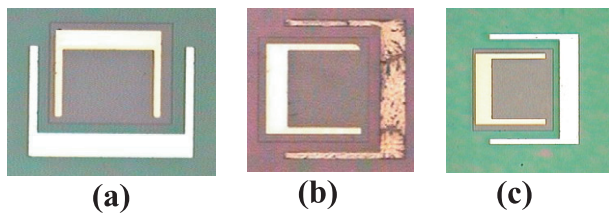


Figure 4. Micrographs of our fabricated n-UV and blue LEDs: (a) with $\lambda_{EL} = 383$ nm, (b) with $\lambda_{EL} = 440$ nm and (c) with $\lambda_{EL} = 452$ nm.

Subsequently, we grow a 690 nm thick, Si doped n-type contact layer. We then continue with the epi-growth of five InGaIn wells and GaN barriers as the active layers of our LEDs. The growth temperature of this active region determines the amount of In incorporation into the wells, which in turn adjusts the emission peak wavelength. Therefore, we use distinct active region growth temperatures for our LEDs. The n-UV LED active layer is grown at 720 °C for 383 nm EL peak, while one of the blue LEDs is grown at 682 °C for 440 nm EL peak and the other blue LED at 661 °C for 452 nm EL peak. Finally, we finish our growth with p-type layers that consist of Mg-doped, 50 nm thick $Al_{0.1}Ga_{0.9}N$ and 120 nm thick GaN layers as the contact cap. Following the growth, we activate Mg dopants at 750 °C for 15 min.

In the device fabrication, we use standard semiconductor processing including photolithography, thermal evaporator (metallization), reactive ion etch (RIE) and rapid thermal annealing. Our p-contacts consist of Ni/Au (15 nm/100 nm) and are annealed at 700 °C for 30 s under N_2 purge. On the other hand, our n-contacts consist of Ti/Al (100 nm/2500 nm) and are annealed at 600 °C for 1 min under N_2 purge. The top-view micrographs of our fabricated n-UV and blue LEDs (with $\lambda_{EL} = 383$ nm in (a), $\lambda_{EL} = 440$ nm in (b) and $\lambda_{EL} = 452$ nm in (c)) are shown in figure 4. For on-chip integration, following the surface treatment, we hybridize the LED top surface with various types of NCs in host polymer. Our n-UV LED and blue LEDs have turn-on voltages approximately at 6 and 4 V, and electroluminescence (EL) peak wavelengths at 383, 440 and 452 nm, respectively, as shown in figure 5.

The operating principle of these hybrid NC-WLEDs relies on the hybrid use of the LED as the pump light source and the integrated NC film as the photoluminescent layer. When electrically driven, the LED optically pumps the NCs. The photoluminescence of these NCs and the electroluminescence

of the LED consequently contribute together to the white light generation. Here with the ability to tune the NC photoluminescence peaks across the visible (using the size effect) and with the right choice of NC combinations, we cover the visible spectrum from blue to red with a necessary spectral power distribution. Furthermore, with the small overlap between the NC emission and absorption spectra, we conveniently modify the white light spectrum as desired with the addition of NCs.

Table 1 lists 26 different samples of our hybrid light sources along with their corresponding tristimulus coordinates, correlated colour temperature and colour rendering index. Sample 1 shows one of the blue LEDs with 452 nm electroluminescence peak as the starting platform. For samples 2–6, we hybridize yellow NCs on this blue LED. In sample 2, we integrate 25 μl NCs in toluene with 3.1 μl PMMA solution corresponding to a concentration of 2.36 $\mu mol ml^{-1}$. For each subsequent sample (from sample 2 to sample 6), we increase the NC solution by multiples of 25 μl and PMMA by 3.1 μl . For sample 6, we end up with 150 μl NC solution and 18.75 μl PMMA, corresponding to a final concentration of 2.36 $\mu mol ml^{-1}$. Consequently, on the CIE chromaticity diagram, the (x, y) tristimulus coordinates of these samples begin with (0.14, 0.03) on the blue edge for 452 nm and reach (0.43, 0.28) in the white region. The correlated colour temperature ranges from cool white colours to warm white colours as we increase the hybridized NCs solution. Furthermore, the colour rendering index starts with -51.5 , increases in each step and reaches 15.8 as a dichromatic source. Therefore, we observe experimentally that the thickness of the hybridized NC thin films significantly shifts the colour parameters of the resulting hybrid LEDs. Figure 6 shows the optical spectrum of sample 6 to observe the increase in the yellow peak with respect to electroluminescence of blue LED.

For samples 7–9, we increase green NC volume in toluene by 25 μl and PMMA by 3.1 μl , corresponding to a concentration of 5.59 $\mu mol ml^{-1}$, and on top of the green NC film we place 150 μl yellow NCs and 18.75 μl PMMA having a concentration of 2.36 $\mu mol ml^{-1}$. As a result, the tristimulus coordinates of these samples move from (0.44, 0.29) to (0.52, 0.37). The corresponding correlated colour temperatures move towards warm white to 1754 K.

When 150 μl yellow NCs and 18.75 μl PMMA with a concentration of 2.36 $\mu mol ml^{-1}$ are hybridized on the blue LED at 452 nm, the colour rendering index is only 15.8 (due to the dichromaticity of the source). However, when 75 μl green NC and 9.3 μl PMMA with a concentration of 5.59 $\mu mol ml^{-1}$ and 150 μl yellow NC and 18.75 μl PMMA with a concentration of 2.36 $\mu mol ml^{-1}$ are hybridized layer by layer in the respective order, the colour rendering index becomes 50.7 (because of the trichromaticity of the source). Figure 7 shows the optical spectrum of this hybrid LED (sample 9). For samples 10 and 11, we similarly observe an increase in correlated colour temperature and colour rendering index by adding red NCs instead of green NCs.

For samples 12–15, we hybridize the cyan NC film first and then add 150 μl yellow NCs and 18.75 μl PMMA having a concentration of 2.36 $\mu mol ml^{-1}$ on top of it. In each sample, we add 25 μl cyan NCs in toluene and 3.1 μl PMMA, corresponding to an additional concentration

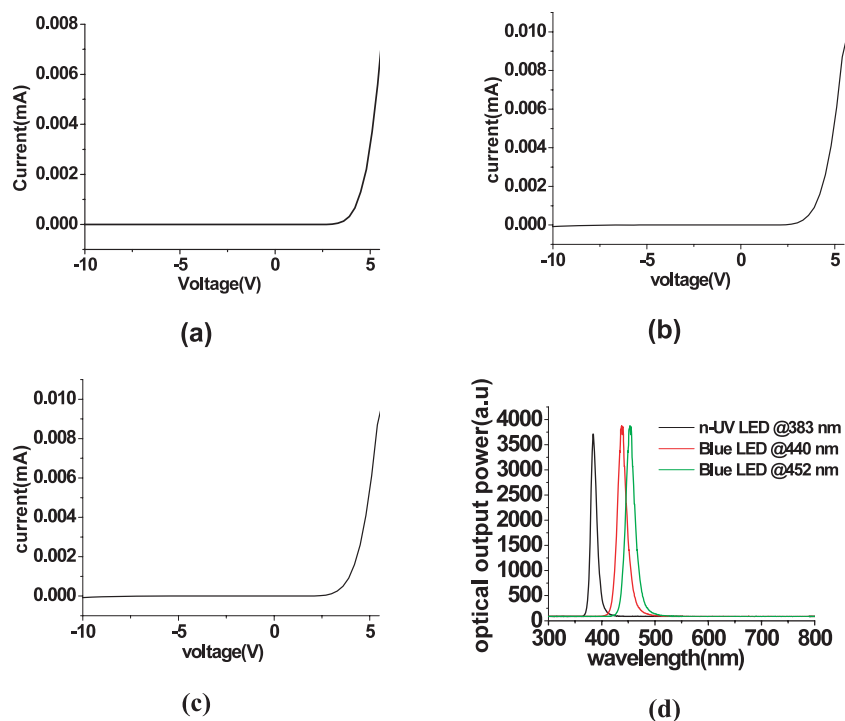


Figure 5. (a) *IV* of n-UV LED ($\lambda_{EL} = 383$ nm), (b) *IV* of blue LED ($\lambda_{EL} = 440$ nm), (c) *IV* of blue LED ($\lambda_{EL} = 452$ nm) and (d) electroluminescence of n-UV LED and two blue LEDs.

Table 1. Our hybrid NC-WLED sample characteristics. (C: cyan NC; G: green NC; Y: yellow NC; R: red NC; * denotes blended NC hybridization.)

Sample #	Hybridized nanocrystals	LED λ_{EL} (nm)	Concentration ($\mu\text{mol ml}^{-1}$)	x	y	T_c (K)	R_a
1	—	452	—	0.14	0.03	34367	-51.5
2	Y	452	2.36	0.15	0.04	34367	-40.2
3	Y	452	2.36	0.16	0.06	34367	-28.6
4	Y	452	2.36	0.20	0.10	34366	-10.1
5	Y	452	2.36	0.24	0.13	34366	-3.8
6	Y	452	2.36	0.43	0.28	1882	15.8
7	G, Y	452	5.59, 2.36	0.44	0.29	1989	37.5
8	G, Y	452	5.59, 2.36	0.45	0.33	2165	54.5
9	G, Y	452	5.59, 2.36	0.52	0.37	1754	50.2
10	R, Y	452	0.88, 2.36	0.57	0.30	1121	42.2
11	R, Y	452	0.88, 2.36	0.62	0.30	1000	50.7
12	C, Y	452	12.05, 2.36	0.24	0.13	34366	-3.4
13	C, Y	452	12.05, 2.36	0.36	0.23	2651	32.4
14	C, Y	452	12.05, 2.36	0.36	0.27	3228	48.3
15	C, Y	452	12.05, 2.36	0.42	0.31	2311	50.2
16	Y	440	0.11	0.37	0.25	2692	14.6
17	C, Y	440	0.37, 0.11	0.37	0.28	3246	19.6
18	G, Y, R	452	0.27, 0.11, 0.025	0.30	0.28	7521	40.9
19	C, G, Y, R	452	0.37, 0.27, 0.1, 0.025	0.24	0.33	11171	71.0
20*	C, Y, R	452	2.54, 0.19, 0.06	0.44	0.26	1625	38.8
21	C, Y, R	452	2.8, 2.8, 2.8	0.20	0.10	34366	1.9
22	C, Y, R	383	2.8, 2.8, 2.8	0.51	0.39	1979	71.9
23*	C, Y, R	383	2.54, 0.19, 0.06	0.61	0.36	1238	74.3
24	C, R	452	2.8, 2.8	0.20	0.11	34367	4.0
25*	C, R	452	2.73, 0.06	0.24	0.13	34366	-13.8
26*	C, R	383	2.73, 0.06	0.57	0.37	1477	47.6
27	C, R	383	2.8, 2.8	0.52	0.41	1977	42.1

of $12.05 \mu\text{mol ml}^{-1}$. By increasing the incorporation of cyan NCs, the tristimulus coordinates move closer to the cyan part of the CIE chromaticity diagram, which would imply

the correlated colour temperature to increase. However, on the contrary, in our samples we observe that the correlated colour temperature of our hybrid NC-LEDs decreases and

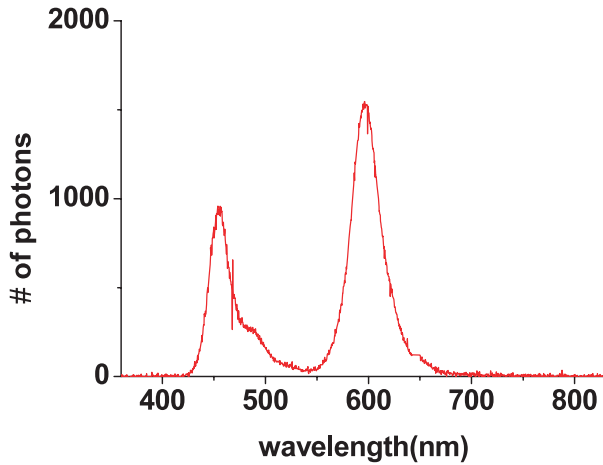


Figure 6. Electroluminescence spectrum of 150 μl yellow NCs ($\lambda_{\text{PL}} = 580 \text{ nm}$) and 18.75 μl PMMA corresponding to a film concentration of $12.05 \mu\text{mol ml}^{-1}$ hybridized on blue LED ($\lambda_{\text{EL}} = 452 \text{ nm}$) measured at an injection current level of 5 mA at room temperature.

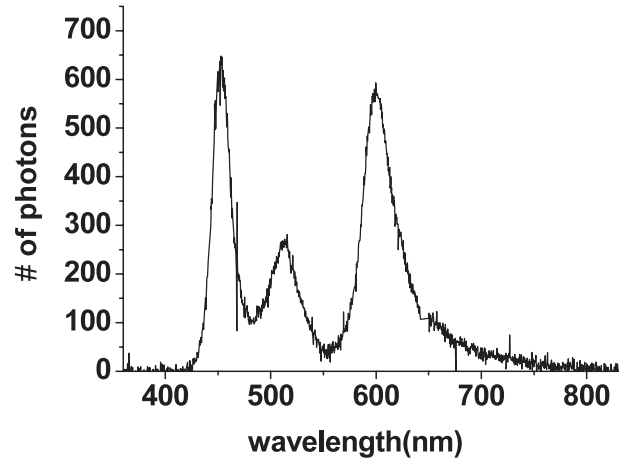


Figure 8. Electroluminescence spectrum of 75 μl cyan NC and 9.3 μl PMMA, corresponding to a film concentration of $12.05 \mu\text{mol ml}^{-1}$, and 150 μl yellow NCs ($\lambda_{\text{PL}} = 500$ and 580 nm) and 18.75 μl PMMA, corresponding to a film concentration of $12.05 \mu\text{mol ml}^{-1}$, hybridized on blue LED ($\lambda_{\text{EL}} = 452 \text{ nm}$) measured at an injection current level of 5 mA at room temperature.

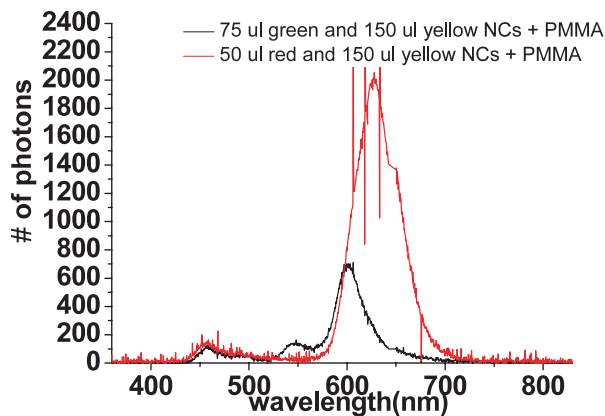


Figure 7. Electroluminescence spectrum of 75 μl green NC and 9.3 μl PMMA corresponding to a film concentration of $5.59 \mu\text{mol ml}^{-1}$ and 150 μl yellow NCs ($\lambda_{\text{PL}} = 540$ and 580 nm) and 18.75 μl PMMA corresponding to a film concentration of $12.05 \mu\text{mol ml}^{-1}$ hybridized with blue LED ($\lambda_{\text{EL}} = 452 \text{ nm}$) at an injection current level of 5 mA and the electroluminescence spectrum of 50 μl red NC and 6.2 μl PMMA corresponding to a film concentration of $0.88 \mu\text{mol ml}^{-1}$ and 150 μl yellow NCs ($\lambda_{\text{PL}} = 620$ and 580 nm) and 18.75 μl PMMA corresponding to a film concentration of $12.05 \mu\text{mol ml}^{-1}$ hybridized on blue LED ($\lambda_{\text{EL}} = 452 \text{ nm}$) measured at an injection current level of 5 mA at room temperature.

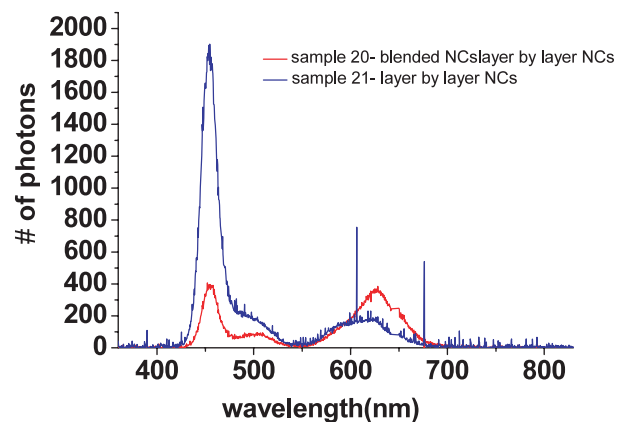


Figure 9. Electroluminescence spectra of samples 20 and 21. Sample 20 consists of a blended mixture of 75 μl cyan NC, 25 μl yellow NC and 25 μl red NC ($\lambda_{\text{PL}} = 540, 580$ and 620 nm) and 2, 6 and 80 μl PMMA mixtures, respectively, corresponding to film concentrations of 2.54, 0.19 and $0.06 \mu\text{mol ml}^{-1}$. Sample 21 consists of layer by layer hybridization of 75 μl cyan NC, 25 μl yellow NC and 25 μl red NC ($\lambda_{\text{PL}} = 540, 580$ and 620 nm) and 88 μl PMMA, corresponding to a film concentration of $2.8 \mu\text{mol ml}^{-1}$, respectively.

becomes a warmer light source. According to our observations, this behaviour stems from the reabsorption of the photons generated by the cyan NCs in the top yellow NC film. Figure 8 shows the optical spectrum of 75 μl cyan and 9.3 μl PMMA corresponding to a concentration of $12.05 \mu\text{mol ml}^{-1}$ and 150 μl yellow NCs and 18.75 μl PMMA having a concentration of $2.36 \mu\text{mol ml}^{-1}$ hybridized on the blue LED with the peak electroluminescence of 452 nm. In table 1, samples 16–19 are also discussed in our previous work [8].

For samples 20–27, we incorporate NCs either blended in a mixture or assembled layer by layer. The samples indicated with * in table 1 are those that are directly hybridized by

blending all the NCs as a mixture and integrated on the LED (rather than placing layer by layer). To compare the optical properties of these two cases, we select samples 20 and 21. Sample 20 consists of blended cyan, yellow and red NCs. On the other hand, for sample 21, we integrate first the red NC film, on top of which comes the yellow NC film and then finally the cyan NC film to prevent the reabsorption of the generated photon by the subsequent films. For each sample, the number of NCs per unit volume (NC concentration) is approximately constant. Figure 9 shows the optical spectrum of both samples 20 and 21. Although the red peak is higher in sample 20, its cyan peak is lower compared to sample 21. This is because the photoluminescence of the cyan NCs has the probability to be reabsorbed by the red and yellow NCs, which reduces

the cyan peak in the blended case in sample 20. Additionally, red and yellow NCs can be further pumped also by the photon emitted from the cyan NCs, increasing the red peak. However, in layer by layer assembly in sample 21, since the cyan NC film is on the top, there is no probability of reabsorption of photoluminescence of cyan NCs.

In conclusion, we demonstrated the hybridization of CdSe/ZnS core-shell nanocrystals on InGaN/GaN based blue/near-UV LED to tune colour properties (tristimulus coordinates, colour correlated temperature and colour rendering index) of the generated light across the visible and within the white region of the CIE chromaticity diagram. Working on 26 samples of hybrid NC-LEDs, we experimentally investigated the effects of NC concentrations and NC film thicknesses on tuning these colour properties and discussed layer by layer assembly of NCs as opposed to blending in a mixture. We concluded that these hybrid white light sources hold great promise for future lighting and display applications with their widely tunable colour properties.

Acknowledgments

This work is supported by EU-PHOREMOST Network of Excellence 511616 and Marie Curie European Reintegration Grant MOON 021391 within the 6th European Community Framework Program and TUBITAK under Project Nos. EEEAG 106E020, 104E114, 105E065, and 105E066.

HVD and SN also acknowledge additional support from the Turkish National Academy of Sciences Distinguished Young Scientist Award and TUBITAK Fellowship programs.

References

- [1] Landau S and Erion J 2007 *Nat. Photon.* **1** 31–2
- [2] Arik M, Petroskf J and Weavery S 2002 *Inter Society Conf. on Thermal Phenomena* pp 112–20
- [3] Nakamura S and Fasol G 1997 *The Blue Laser Diode* (Berlin: Springer)
- [4] Schubert E F 2006 *Light-Emitting Diodes* (Cambridge: Cambridge University Press)
- [5] Yamada M, Narukawa Y, Tamaki H, Murazaki Y and Mukai T 2005 *IEICE Trans. Electron.* **E88–C 9** 1860–71
- [6] Zukauskas A, Shur M S and Gaska R 2001 *MRS Bull.* **26** 764–9
- [7] Heliotis G, Gu E, Griffin C, Jeon C W, Stavrinou P N, Dawson M D and Bradley D D C 2006 *J. Opt. A: Pure Appl. Opt.* **8** 445–9
- [8] Nizamoglu S, Ozel T, Sari E and Demir H V 2007 *Nanotechnology* **18** 065709
- [9] Nizamoglu S, Ozel T, Sari E and Demir H V 2006 *IEEE COMMAD Conf. on Optoelectronic and Microelectronic Materials and Devices (Perth, Australia)* WO-A5
- [10] Chen H, Yeh D, Lu C, Huang C, Shiao W, Huang J, Yang C C, Liu I and Su W 2006 *IEEE Photon. Technol. Lett.* **18** 1430–2
- [11] Chen H, Hsu C and Hong H 2006 *IEEE Photon. Technol. Lett.* **18** 193–5
- [12] Petruska M A, Koleske D D, Crawford M H and Klimov V I 2006 *Nano Lett.* **6** 1396–400